Fabrication and Optical Characterization of Poly(2,5-di-*n*-butoxyphenylene) Nanofibril Arrays

Bozhang Yu, Yuan Gao, Hulin Li

Department of Chemistry, Lanzhou University, Lanzhou 730000, People's Republic of China

Received 30 August 2001; accepted 21 April 2003

ABSTRACT: Anodic aluminum oxide (AAO) membrane can be used as template for the synthesized nanostructures. In this article, we have prepared the AAO membrane by using electrooxidation of aluminum substrate in phosphoric acid, and fabricated poly(2,5-di-*n*-butoxyphenylene) (BuO–PPP) nanofibril arrays by oxidative coupling polymerization of 1,4-di-*n*-butoxybenzene (DBB) within the pores of the AAO template membrane. The detailed molecular structure of the polymer nanofibrils was characterized by using infrared and ^{1}H nuclear magnetic resonance spectra, and estimated to consist of almost equal fractions of 1,4- and 1,3-linkages. We have used transmission electron microscopy, scanning electron microscopy, and atom force microscopy to confirm the morphologies and images of the AAO template membrane and the fabricated nanometer scale of BuO–PPP nanofibril arrays. The experimental results demonstrated that the pores of the AAO membrane were regular and uniform, and parallel each other, and the BuO–PPP chains in the narrowest template-synthesized nanofibrils were oriented parallel to the porous axes of the AAO membrane and perpendicular to the surface of the aluminum substrate. The polymer chain orientation was partially responsible for the enhanced conductivity. The ultraviolet absorption spectrum of the BuO–PPP nanofibril arrays shown that the polymer contains a better extended π-conjugation system along poly(*p*-phenylene) backbone, which resulted in longer wavelength shift of the absorption band, the absorption maxima were located at 258 nm (E_1 absorption band) and 332 nm (E_2 absorption band), respectively. Photoluminescence spectrum of the BuO–PPP nanofibril arrays exhibited a blue emission. © 2003 Wiley Periodicals, Inc. J Appl Polym Sci 91: 425–430, 2004

Key words: polyaromatics; morphology; nanocomposites; templates; spectroscopy

INTRODUCTION

High regular patterned arrays of nanostructures have numerous potential applications in construction of novel type of optoelectronic and magnetic device,[1–4] drug delivery,[5] and bioencapsulation.[6] The template synthesis method is used to prepare a desired material within the nanoporous membranes, and these nanoarrays have versatile interesting and useful characteristics, including tubules, fibrils, and wires of electronically conductive polymer,[7–10] metals,[11–13] semiconductor.[14–16] It has been discovered that the template-synthesized materials have unique supermolecular feature of electrochemical, electronic, optical absorption, and enhanced conductivity.[8] The types of the porous membranes includes usually track-etch polymeric membranes, such as polycarbonate and polyester membranes,[17,18] and porous aluminum membranes.[19,20] The track-etch membranes contain cylindrical pores of uniform diameter, and the membranes with a wide range of the diameters and densities of the pores approaching 10^9 pore/cm^2 are available commercially. The pores in the anodic aluminum oxide membrane are arranged in a regular hexagonal array, and grow perpendicular to the aluminum substrate with narrow distribution of porous spaces. The porous AAO membrane has been widely used as the template for construction of regular nanoarrays, in which nanofibrils within the pores are also mutually parallel and aligned perpendicular to the aluminum substrate[19–21]; these nanomaterials can be freed from the template membrane and collected.

With the development of synthesis and application of novel polymer material, the design and construction of organic nanopolymer have become a great interest.[22,23] The conductive polymer chains contain a conjugated system, such as polyacetylene, polypyrrole, polythiophene, and polyaniline, and they have copious charge carriers and enhanced electronic conductivity by oxidizing or reducing polymer,[18,24] i.e., "by means of doping." The doped polyacetylenes are so reactive that it appears unlikely that the polymer will be useful for any of proposed applications of conductive polymers. Although polypyrrole and polyaniline are more chemically stable materials, their conductivity is many orders of magnitude lower.[25] The template synthesis method provides a route for improving the conductivities of these polymers.[26,27]

Correspondence to: H. Yi (lihl@lzu.edu.cn).

Contract grant sponsor: National Nature and Science Foundation of China (NNSF).

Martin et al. have prepared polypyrrole, poly(3-methylthiophene), and polyaniline either chemically or electrochemically in the pores of the polycarbonate membranes, it was demonstrated that the polymer chains preferentially nucleate and grow on the pores walls of the template, and the polymers with enhanced molecular and supermolecular order contain fewer conjugation-interrupting defects, such as sp^3-hybridized carbons or twists and kinks in the polymer chains, For polypyrrole, the polymeric tubules or solid fibrils are obtained by controlling the polymerization time, but polyaniline tubules will not close up.[31] In past decades, poly(*p*-phenylene) (PPP) and some derivatives have been used as electrode materials in electrochemical cells, and blue-emitting diodes.[32–34] But the poly(*p*-phenylene) prepared by oxidative coupling polymerization is insoluble in all solvent and inflexible.[35] Introduction of flexible side chains into the aromatic rings can not only render solubility and processibility, but also improve their optical and electrical properties.[36,37] In recent years, the fabrication of poly(2,5-di-n-butoxyphenylene) nanofibril arrays have not been reported; in this article, we present the fabrication and morphology of uniform poly(2,5-di-n-butoxyphenylene) nanofibril arrays by using the AAO template-synthesized method. It is found that the polymer nanofibrils contain a better extended π-conjugation system along the poly(*p*-phenylene) backbone. The uniform large area arrays reveal a blue emission. We infer that the polymer chains in the narrowest nanofibrils are oriented parallel to the axes of these nanofibrils by measuring the dc conductivity of the BuO–PPP nanofibril arrays.

EXPERIMENTAL

Materials

Reagent grade anhydrous $FeCl_3$ was purified by sublimation. Chloroform was purified by washing sequentially with sodium phenolate, water, concentrated sulfuric acid, diluted aqueous base, and water, followed by drying anhydrous sodium sulfate, and distillation. The 1,4-di-*n*-utoxybenzene was prepared by the reaction of hydroquinone with *n*-butyl bromide in alkaline solution. Recrystallization from water–methanol gave white plates (yield 80%); mp: 43–45°C; infrared (IR) (KBr): ν3050 and 2960–2870 (C—H), 1510 and 1480 (C═C), 1230 cm^{-1} (C—O—C). Anal. Calcd. for $C_{14}H_{22}O_2$: C, 75.63, H, 9.97. Found: C, 75.70, H, 9.71.

Fabrication of AAO template

The AAO template membrane was prepared according to our previous procedure.[19,20] Aluminum foil (99.99%, 1.0 × 20 × 30 mm^3) was first degreased in ultrasonic baths of trichloroethylene, and etched in 1.0 mol · L^{-1} sodium hydroxide, and then cleaned thoroughly with distilled water. Next, we have it electropolished in a mixed solution of perchloric acid and alcohol, and rinsed with distilled water. The obtained aluminum foil was anodized at 90 V in 0.5 mol · L^{-1} phosphoric acid by using two lead foils as cathode. The sample was rinsed thoroughly with distilled water, and dried in a stream of nitrogen.

Fabrication of BuO–PPP nanofibril arrays

The reaction was carried out under argon atmosphere in a 250 mL three-neck flask. First, anhydrous $FeCl_3$ (6.48 g) and drying chloroform (30 mL) were placed in the flask, after it was vacuumized continuously three times and filled with argon; the dried chloroform (30 mL) containing 1,4-di-n-butoxybenzene (2.22 g) and the AAO templates were added into it by using syringe. The mixture was slowly stirred at room temperature; BuO–PPP was produced from the monomer (DBB) and deposited within the pores of the AAO membrane during this period. After 24 h, the solidified mixture and the AAO template were poured into methanol, and refluxed for 2 h, and then dried in vacuum at 80°C. It was found that the DBB was polymerized within the pores and on both faces of the AAO template membrane, the poly(2,5di-n-butoxyphenylene) nanofibril arrays were light brown, and soluble even in tetrahydrofuran and tetrachloromethane at room temperature. The powderous polymer can be also prepared in the light of the same identical conditions as the synthesized BuO–PPP fibril arrays without using the AAO template.

Sample preparation for measurement of AFM and optical properties

The AAO membrane filled with the BuO–PPP was plunged into tetrachloromethane solution in order that the polymer nucleated on the AAO membrane surface was removed. The exposed boundaries of the AAO membrane were slightly dissolved in 0.5mol · L^{-1} sodium hydroxide, and the BuO–PPP nanofibril arrays within the AAO membrane was revealed from the bottom to the top, the sample was repeatedly washed by distilled water, and dried in the air.

Sample preparation of DC conductivity measurements

The BuO–PPP/AAO nanocomposite membranes (20 × 30 mm) were immersed in saturated mercuric chloride solution, and stripped from aluminum substrate. The pores of the stripped AAO membrane were enlarged in 0.5mol · L^{-1} phosphoric acid so that the pores were made open from the top to the bottom. The

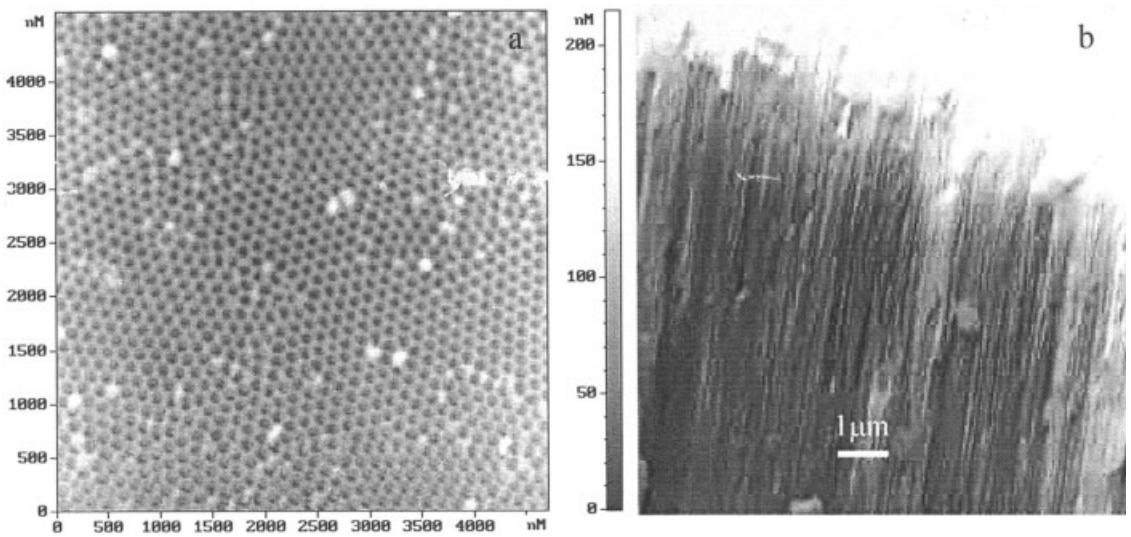

Figure 1 (a) The AFM image of the AAO template. (b) The TEM section cross image of the AAO template prepared by electrooxidation of aluminum substrate in phosphoric acid.

sample was washed with distilled water, and dried in the air. Finally, an aluminum film was sputtered on the BuO–PPP nanofibrils surface, its thickness is about 0.2 μm. The resistance of the nanocomposite membranes was measured with two probes method by using high-resistance meter. For the dc conductivity of the powderous poly(2,5-butoxyphenylene), the BuO–PPP powder was pressed into pellets under a pressure of 2×10^6 kg/cm^2, the same conductivity surveying method as the BuO–PPP nanofibril arrays was used.

Measurements

The infrared spectrum was recorded with Nicolet AVATAR 360 FIIR spectrometer. The ultraviolet spectrum was obtained by TU-1901 spectrometer in tetrachloromethane. The ^{1}H-NMR (nuclear magnetic resonance) spectrum was made with Brüker AM 400 NMR spectrometer. The TEM pattern was carried on JEM-1200 EX-/S (9100 EDAX)(75KV). The AFM surface images were measured by using P47-SPM-MDT (made in Russia). The photoluminescence (PL) spectra were obtained by Shimadizu RF-540 spectrometer. The high-resistance meter was used to measure dc conductivity of the BuO–PPP nanofibril arrays.

RESULTS AND DISCUSSION

Figure 1(a) shows the AFM surface image of the AAO template membrane prepared by electrooxidation in phosphoric acid. Ones note that the pore size within the AAO template membrane is about 150 nm, the nanopores are separated from each other, and high regular and uniform arrangements, and then the densities are about 10^{11} pores/cm^2. Figure 1(b) is the SEM section cross image of the AAO membrane, it shows that the porous length is about 10 μm, and its aspect ratio (length/diameter) is about 60. These pores are parallel and perpendicular to aluminum substrate; the AAO membranes would allow a great number of nanostructures to be produced per unit area of the template. Figure 2 indicates the TEM image of the BuO–PPP nanofibrils liberated from the AAO template membrane by dissolving the aluminum layer with sodium hydroxide, they was not tubules but

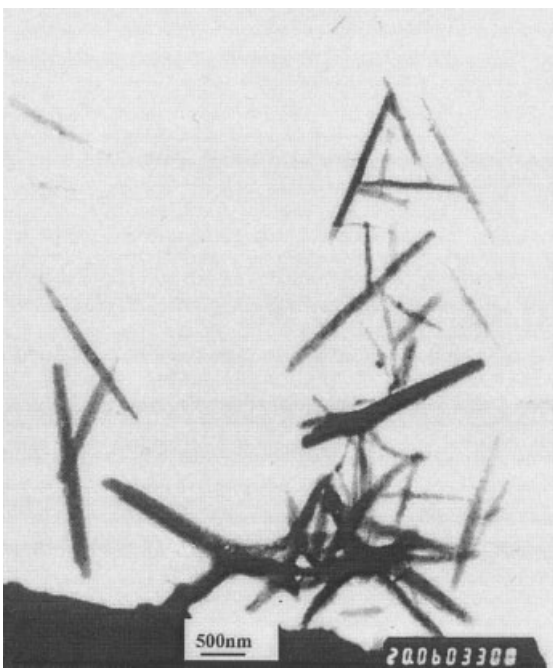

Figure 2 The TEM image of the BuO–PPP nanofibril arrays prepared by the AAO template-synthesized method.

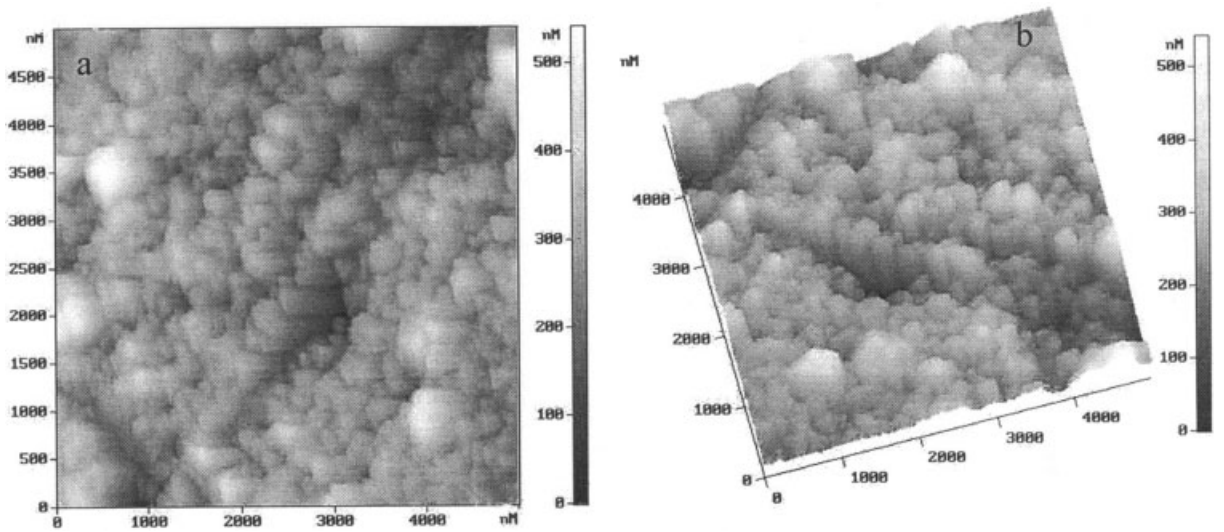

Figure 3 (a) The AFM image of the BuO–PPP nanofibril arrays. (b) The three-dimensional AFM image of the BuO–PPP nanofibril arrays by slightly dissolving the AAO membrane

solid fibrils, and some nanofibrils are broken, but the BuO–PPP structure was not changed. It is postulated that the polymer preferentially nucleates and grows on the porous walls of the AAO membrane, and ultimately close up to form solid fibrils, the aspect ratio of the BuO–PPP nanofibrils is in agreement with that of the AAO membrane template.[28,29] Figure 3(a) exhibits the AFM surface image of the BuO–PPP nanofibril arrays obtained by slightly dissolving the BuO–PPP/AAO composite membranes, it demonstrates that the BuO–PPP nanofibrils can grow in pores of AAO membrane separately from each other, and they must be high regular and uniform arrangements that protrude from the top surface of the dissolved AAO membrane. Because the pores of the AAO membrane are regular and uniform, after the nanopores are filled with the BuO–PPP chains, and polymer nanofibril arrays are formed into the pores, the obtained BuO–PPP nanofibrils can also take on highly regular and uniform arrays in consistent with the surface image of the AAO template membrane, as shown in Figure 1. One also finds that some lacuna appear in the AFM image: on the one hand, this can relate to dissolving the BuO–PPP of the AAO membrane surface; on the other hand, the AAO nanoporous walls are rather thinner, and the porous boundaries can be easily dissolved in sodium hydroxide solution. This process can make the AAO membrane surface depressed, and partial nanofibrils were broken. Figure 3(b) shows the three-dimensional AFM image of the BuO–PPP nanofibril arrays; it is discovered that the BuO–PPP nanofibrils can reveal from pores of the AAO membrane—the average height of the revealed nanofibrils is about 350 nm from the bottom to the top. Beyond this height, the polymer aggregated on the surface of the AAO membrane would emerge with the BuO–PPP nanofibril arrays within the pores membrane. The experimental evidence indicates that the BuO–PPP can be imbedded within the pores of the AAO membrane to give uniform nanofibril arrays, in which these nanofibrils are insulated to each other. Such template synthesis method provides the best control to the shape of the BuO–PPP nanofibrils. All above unique properties make such arrays applied in optical device.

The self-assembling process of the BuO–PPP nanofibril arrays in the host template can include chemadsorption and oxidation steps. The first step is a one-electron oxidation of the aromatic nucleus to give a cation radical, which attacks the aromatic ring of a second molecule to yield dihydro radical-cation species. Meanwhile, a cation radical and/or dihydro radical cation can be adsorbed on the porous AAO wall. This species releases a proton to form a radical that undergoes a further oxidation followed by proton loss to give the dimerization product. The cation radical further attacks the dimerization; the oxidative coupling polymerization was continuously carried out in the AAO interpores. The high dielectric constant of the AAO template at the same time could reduce repulsion between the positive charges in oxidative polymerization,[32–34] and subsequently volume expansion of nanofibers can expel inorganic salts from the nanoporous aluminum oxide.[38,39]

In order to understand the polymer chains preferentially nucleate on the walls of pores, we consider the effect of oxygen deficit of the AAO membrane on adsorption of cation radical and/or dihydro radical-cation species. The oxygen deficit indicates that hydroxy and oxygen anions exist in the porous surface of the AAO membrane, and can adsorb intermediate of the cation radical so that the polymer chains preferentially aggregate along the porous walls of the AAO

membrane. By measuring dc conductivity, we note that both are different between the BuO–PPP/AAO composite membranes and powderous polymer. For the BuO–PPP/AAO composite membranes, the dc conductivity is about 5.96×10^{-8} S · cm^{-1}, and the latter is only 6.25×10^{-1} S · cm^{-1}. It is reasonable to postulate that the aggregation effects play an important role in the polymeric dc conductivity. This demonstrates that the conjugated defects of the BuO–PPP chains in pores of the AAO membrane are less. It can be believed that the polymer chains are oriented parallel to the porous axes of the AAO membrane, and ultimately close up to form solid nanofibrils, the aspect ratio of the BuO–PPP nanofibrils should also be consistent with that of the AAO template.

The IR spectrum of the liberated BuO–PPP nanofibrils in tetrachloromethane exhibited the characteristic absorption at 2960–2870, 1490, and 1205 cm^{-1} due to C—H, C═C, and C—O—C stretching, respectively. The absorption at 865cm^{-1} attributed to the C—H out-of-plane vibration of tetrasubstituted benzene. The absorption band assigned to hydroxyl group at 3600 cm^{-1} was not observed. Values from elemental analysis of the BuO–PPP condensed were in good agreement with the calculated ones.

The oxidative coupling polymerization of 1,4-di-n-butoxybenzene will be expected to give 1,3- and 1,4-linkage. ^{1}H-NMR spectrum of the BuO–PPP nanofibrils dissolved in $CDCl_3$ indicated five intense absorptions at 0.89, 1.39, 1.66, 4.01, and 7.09 ppm, respectively, due to the methyl, γ-methylene, β-methylene, and α- methylene protons of the alkoxy group and aromatic protons, these ascribed to the formation of 1,4-linkage. Furthermore, extra weak but well-defined signals were observed at 4.05, 7.5, and 7.6; the 4.05 ppm resonance may be assigned to the α- methylene protons of the alkoxy group. The resonances near 7.5 ppm arise from the phenyl protons in mixed connectivities. From the relative integration of signals with protons, it is estimate that the percentage of 1,3-linkage is about 50%.

Figure 4(a) shows the ultraviolet absorption spectrum of the BuO–PPP nanofibril arrays liberated in sodium hydroxide. The maximum absorption peaks are located at 258 nm (E_1 absorption band) and 332 nm (E_2 absorption band), respectively. However, the ultraviolet absorption maximum of 1,4-butoxybenzene locates at 285 nm. The position of the polymer absorption reveals a better extended π-conjugation system along the poly(*p*-phenylene) backbone, which brings on 32 nm bathochromic shift of the E_2 absorption band in comparison with that of poly(*p*-phenylene). The energy gap (E_g) of π to π^* transition calculated by absorptive edge is about 3.3 eV, and is about 0.3 ~0.6 eV larger than that of poly(*p*-phenylene).[32,33] By adding electron donating *n*-butoxy groups, the energy gap can be influenced by the BuO–PPP structure. First, the

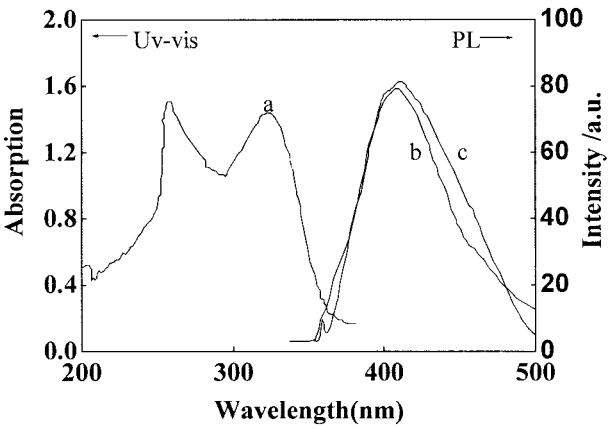

Figure 4 (a) The ultraviolet absorption spectrum of the BuO–PPP nanofibril arrays within the AAO membrane. (b) The photoluminescence spectrum of the BuO–PPP nanofibril arrays by slightly dissolving the AAO membrane. (c) The photoluminescence spectrum of the BuO–PPP nanofibril dissolved in TCM.

butoxy groups increase electron densities, which makes energy gap of the BuO–PPP decreased. Second, the steric hindrance of the butoxy groups has the effective conjugated chain reduced so that the energy gap of the BuO–PPP nanofibrils increases. In the photoluminescence measurement, all the measurements were carried out in the air, the excitation wavelength of the BuO–PPP nanofibril arrays liberated in sodium hydroxide was 356 nm, and its emission peak appeared at 416 nm, as shown in Figure 4(b). Figure 4(c) shows the photoluminescence spectrum of the dilute solution of the BuO–PPP nanofibrils in tetrachloromethane, the excitation peak located at 357 nm, and the emission maximum situated at 420 nm. The emission intensity peak of the dilute polymer solution is slightly stronger than the nanofibril arrays, and the peak shape is analogous to that of the BuO–PPP nanofibril arrays. In comparison with the emission peaks of the dilute BuO–PPP solution, it could be found that there is a further 4 nm blue shift for the BuO–PPP nanofibril arrays, but it remains in the blue range of the spectrum. The blue-shift phenonmenon could be caused by the quantum size effect owing to the highly porous density of the AAO template. Furthermore, the ambient dielectric constant of the nanofibril arrays is different from the BuO–PPP nanofibrils in tetrachloromethane, the twists of the polymer chains in the dilute solution cause conjugation-interrupting defects,[27–29] these factors can also influence emission wavelength, the detailed reason for this change needs further research.

CONCLUSION

Our studies indicate that the BuO–PPP nanofibril arrays can be readily fabricated by oxidative coupling

polymerization of 1,4-di-*n*-butoxybenzene into the AAO template. The detailed molecular structure was characterized by using IR and ^{1}H-NMR spectra, and estimate to consist of 1,3- and 1,4-linkage. The BuO–PPP nanofibrils arrays are high regular and uniform, and their average height is about 350 nm. The polymer chains within the nanofibrils are oriented parallel to the axes of these fibrils and the AAO template so that this decreases conjugation-interrupting defects caused by twists and kinks of the BuO–PPP conjugated chains, and it can make the dc conductivity of the polymer nanofibrils enhanced. In the template synthesis process, the nascent BuO–PPP preferentially nucleates on the porous walls due to having oxygen deficit into the AAO membrane. An analogous aggregation phenomenon has been observed into polycarbonate membrane.[29,40] The ultraviolet absorption spectrum demonstrates that the polymer chains have a better extended π- conjugation system along the poly(*p*-phenylene) backbone. There is a blue emission for the BuO–PPP nanofibril arrays due to the higher porous densities of the AAO membrane, this is a more convenient way for low-cost flat panel displays.

References

1. Zhu, T.; Yu, H. Z.; Wang, J.; Cai, S. M.; Liu, Z. F. Chem Phys Lett 1997, 265, 334.
2. Tarabara, V. V.; Nabiev, I. K.; Feofanov, A. V. Langmuir 1998, 14, 1092.
3. Fulishima, A.; Honda, K. Nature 1972, 37, 238.
4. Whitney, T. M.; Jiang, J. S.; Searson, P. C.; Chien, C. L. Science 1993, 261, 1316.
5. Gref, R.; Minamitake, M.; Perachia, T.; Trubetskoy, V.; Torchilin, V.; Langer, R. Science 1994, 263, 1600.
6. Parthasarathy, R. V.; Martin, C. R. Nature 1994, 369, 298.
7. Martin, C. R.; Van Deke, L. S.; Cai, Z.; Liang W. J. J Am Chem Soc 1990, 112, 8976.
8. Liang, W. J.; Martin, C. R. J Am Chem Soc 1990, 112, 9666.
9. Penner, R. M.; Martin, C. R. J Electrochem Soc 1986, 133, 2206.
10. Martin, C. R.; Parthasarathy, R. V.; Menon, V. Synth Met 1993, 55, 1165.
11. Menon, V. P.; Martin, C. R. Anal Chem 1995, 67, 1920.
12. Foss, C. A., Jr.; Tierney, M.; Martin, C. R. J Phys Chem 1992, 96, 9001.
13. Foss, C. A., Jr.; Hornyak, G. L.; Stockert, J. A.; Martin, C. R. J Phys Chem 1992, 96, 7497.
14. Nishizawa, M.; Menon, V. P.; Martin, C. R. Science 1995, 268, 700.
15. Lakshimi, B. B.; Dorhout, P. K.; Martin, C. R. Chem Mater 1997, 9, 857.
16. Klein, J. D.; Herrick, R. D. I.; Palmer, D.; Sailor, M. J.; Brunlik, C. J.; Martin, C. R. Chem Matter 1993, 5, 902.
17. Martin, C. R. Acc Chem Res 1995, 28, 61.
18. Hulteen, J. C.; Martin, C. R. J Mater Chem 1997, 7171, 1075.
19. Pan, S. L.; Zeng, D. D.; Zhang, H. L.; Li, H. L. Appl Phys A 2000, 70, 637.
20. Peng, Y.; Zhang, H. L.; Pan, S. L.; Li, H. L. J Appl Phys 2000, 7, 87.
21. Yu; B. Z.; Li, H. L. Mater Sci Eng A 2002, 325, 215.
22. Liu, G.; Ding, J.; Hashimoto, T.; Saijo, K.; Wiik, F. M.; Nigam, S. Chem Mater 1999, 11, 2233.
23. Stewart, S.; Liu, G. Chem Mater 1999, 11, 1048.
24. Penner, R. M.; Van Dyke, L. S.; Martin, C. R. J Phys Chem 1988, 92, 5274.
25. Miller, J. S. Adv Mater 1993, 5, 587.
26. Naarmann, H.; Theophilou, N. Synth Met 1987, 22, 1.
27. Lei, J.; Cai, Z.; Martin, C. R. Synth Met 1992, 46, 53.
28. Lei, J.; Menon, V. P.; Martin, C. R. Polym Adv Technol 1992, 4, 124.
29. Cai, Z.; Martin, C. R. J Am Chem Soc 1989, 111, 4138.
30. Martin, C. R. Adv Mater 1991, 3, 457.
31. Parthasarathy, R. V.; Martin, C. R. Chem Mater 1994, 6, 1627.
32. Grem, G.; Martin, V.; Meghdad, F.; Paar, C.; Slampft, J.; Sturm, J.; Tasch, S.; Leising, G. Synth Met 1995, 71, 2193.
33. Grem, G.; Leditzky, G.; Ullrich, B.; Leising, G. Adv Mater 1992, 4, 36.
34. Kovacic, P.; Jones, M. B. Chem Rev 1987, 87, 357.
35. Kovacic, P.; Kyriakis, A. J Am Chem Soc 1963, 85, 454.
36. Ueda, M.; Abe, T.; Awano, H. Macromolecules 1992, 25, 5125.
37. Kada, T.; Ogata, T.; Ueda, M. Macromolecules 1996, 29, 7645.
38. Jessensky, O.; Muller, F.; Gosele, U. Appl Phys Lett 1998, 72, 1173.
39. Jessensky, O.; Muller, F.; Gosele, U. J Electrochem Soc 1998, 145, 3735.
40. Gregory, R. V.; Kimbrel, W. C.; Kuhn, H. H. Synth Met 1989, 28, C823.